Temporal contrast degration due to spectral phase distortion in CPA lasers

Qingwei Yang (杨庆伟)[1*], Mingwei Liu (刘明伟)[2], Yanhai Wang (王艳海)[3], Xinglong Xie (谢兴龙)[1], Jun Kang (康 俊)[1], Meizhi Sun (孙美智)[1], Tingting Xu (徐婷婷)[1], Qi Gao (高 奇)[1], Ailin Guo (郭爱林)[1], and Zunqi Lin (林尊琪)[1]

[1]*National Laboratory on High Power Laser and Physics, Shanghai Institute of Optics and Fine Mechanics, Chinese Academy of Sciences, Shanghai 201800, China*

[2]*School of Physics, Hunan University of Science and Technology, Xiangtan 411201, China*

[3]*College of Sciences, Hebei University of Science and Technology, Shijiazhuang 050018, China*

[*]*Corresponding author: yqwphy@siom.ac.cn*

Received April 1, 2012; accepted July 23, 2012; posted online September 23, 2012

We theoretically study the temporal contrast degradation by the spectral phase distortion in chirped pulse amplification (CPA) lasers. As an example, we analyze the impact of the surface qualities of the optical elements such as mirrors and grating in the stretcher and compressor on the temporal contrast. The temporal contrast declines fast in the case of a rapidly varying random surface error of the optical elements. When the values of PV, RMS and GRMS of the surface error curve are reduced, the temporal contrast is becoming better and better. And the temporal contrast can be improved after the surface error curve is to be spatial filtering. Those results are helpful for the choice of the surface parameters of the optical elements in the stretcher and compressor.

OCIS codes: 140.7090, 320.5520, 320.5390.

doi: 10.3788/COL201210.S21401.

In the chirped pulse amplification (CPA) laser system[1], the temporal contrast between the main pulse and prepulses is an important factor[2]. The peak laser intensity up to 10^{22} W/cm^2 is now achievable and is expected to boost to 10^{24} W/cm^2 in the near future[3]. However, in the application of a high-intensity laser to solid-target experiments, the 10^{10}-W/cm^2 prepulse is strong enough to generate unwanted plasmas before the main pulse arrives on the target and modify the target conditions[2]. So it is important to develop higher temporal contrast in CPA laser system.

There are many temporal contrast-limiting factors[4−7], such as amplified spontaneous emission (ASE), spectral chipping, residual high-order dispersion, spectral phase distortion, etc. In this letter, we focus on the temporal contrast degradation by the spectral phase distortion in CPA lasers. As an example, we analyze the impact of the surface qualities of the optical elements such as mirrors and grating in the stretcher and compressor on the temporal contrast.

In a stretcher or compressor, the surface qualities of the optical elements such as mirrors and grating are very important for the spectral phase noise. Because the laser beam in the stretcher and compressor is spectrally resolved. Therefore, the roughness of the surface in the stretcher and compressor is directly converted to the spectral phase noise, which reduces the temporal coherence of the main pulse and generates a noisy structure on its sides[8].

The pulse contrast is associated with the temporal distribution of the normalized laser intensity. The final output pulse contrast can be given by

$$I(t) = \left| \frac{1}{2\pi} \int_{\omega_1}^{\omega_2} A_{\text{output}}(\omega) \exp\left[-\mathrm{i}\omega t + \mathrm{i}\phi(\omega)\right] \mathrm{d}\omega \right|^2, \quad (1)$$

where $\omega_1 = 2\pi c/\lambda_1$, $\omega_2 = 2\pi c/\lambda_2$, λ_1 and λ_2 are the maximum and the minimum values of λ determined by the laser system, c is the speed of light in vacuum, and $A_{\text{output}}(\omega)$ is the pulse spectral function out of the compressor.

In general, the expression of $\phi(\omega)$ can be written as

$$\phi(\omega) = \phi_{\text{RD}}(\omega) + \phi_{\text{SQ}}(\omega), \quad (2)$$

where

$$\phi_{\text{RD}}(\omega) = \phi_0(\omega) + \phi^{(1)}(\omega_0)(\omega - \omega_0) + \frac{1}{2}\phi^{(2)}(\omega_0)(\omega - \omega_0)^2 + \cdots, \quad (3)$$

is residual dispersion of the laser system;

$$\phi_{\text{SQ}}(\omega) = \frac{2\pi L(x)}{\lambda}, \quad (4)$$

is the phase distortion caused by surface qualities of the optical elements in the stretcher and compressor, in which $L(x)$ is surface error curves of the optical elements and x is the horizontal space.

To demonstrate the temporal contrast degration due to spectral phase distortion in CPA laser, we take the parameters used in the SG II laser system[9] as examples. The chirped ratio is $C_{\text{R}} = 3.2$ ns/6.5 nm, making use of multi-layer dielectric gratings with $N = 1\,740$ mm^{-1}. The widths of the gratings are $W_a = 940$ mm and $W_b = 1\,220$ mm. The incident angle is $\gamma = 70°$. The central wavelength is $\lambda_0 = 1\,053$ nm, while the minimum and the maximum values are $\lambda_1 = 1\,043.5$ nm and $\lambda_2 = 1\,062.5$ nm. For simplicity, we neglect the influence of the residual high order dispersion, i.e., $\phi_{\text{RD}}(\omega) = 0$. Moreover, the pulse spectral

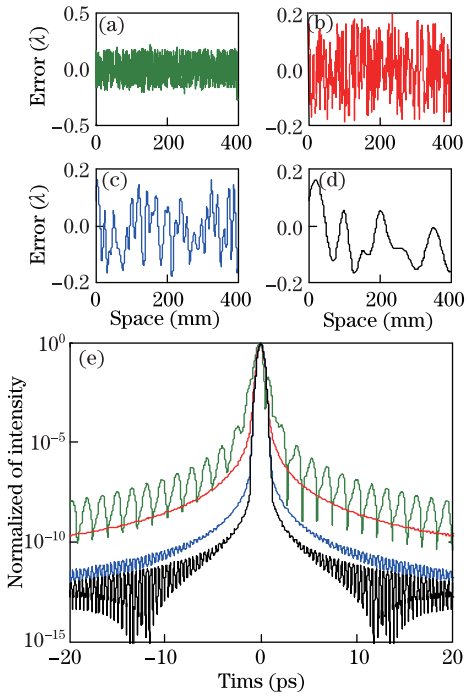

Fig. 1. (Color online) (a)–(d) Different surface error curves of the optical elements in the stretcher and compressor. (e) The temporal distribution of the normalized laser intensity corresponding to the surface error curves in (a)–(d).

function out of the compressor is assumed to be expressed with the fundamental Gaussian function. Then the output pulse spectral function can be written as

$$A_{\text{output}}(\omega) = \exp[-\tau^2(\omega-\omega_0)^2/(8\ln 2)], \qquad (5)$$

where $\omega_0 = 2\pi c/\lambda_0$ and $\tau = 0.5$ ps is the pulse width (full-width at half-maximum (FWHM)).

To qualitatively analyze the temporal contrast degration by surface error curves of the optical elements in the stretcher and compressor, the surface error curves of the optical elements are assumed to be a arbitrary random function. For simulations, different surface error curves of the optical elements are generated by function "random" in the matlab software. And the different frequencies of the surface error curves are achieved by different interpolations in generated random surface error curves.

Figures 1(a)–(d) plot different surface errors curves of the optical elements in the stretcher and compressor, and the corresponding temporal contrasts are shown in Fig. 1(e). The peak-to-valley (PV) is assumed to be $\lambda/3$. As shown in Fig. 1(e), with the same value of PV, the temporal contrast declines fast in the case of a rapidly varying random error. And the temporal contrast hardly changes when the random error curve changes slowly.

In order to further quantitatively analyze the temporal contrast degration by surface error curves of the optical elements in the stretcher and compressor, the surface error curves of the optical elements are assumed to be a Gaussian gradient distribution. For simulations, a random Gaussian phase screen is used for generating a Gaussian gradient distribution[10].

Then the surface error curves of the optical elements in the stretcher and compressor are

$$L(x) = \frac{\lambda}{m} \cdot \text{random}[-1:1] * \exp\left[-\left(\frac{x}{S_{\text{g}}}\right)^2\right], \qquad (6)$$

where $\lambda = 633$ nm, m is the parameter of controlling PV, random$[-1:1]$ is a random function for generating a random number between –1 to 1, S_{g} is the surface error scale, and $*$ is represented convolution.

Figures 2(a)–(d) plot different surface error curves of the optical elements generated by random phase screen in the stretcher and compressor. In Fig. 2(a)–(d), the surface error curves are achieved by using following parameters: (a) $m = 5$, $S_{\text{g}} = 6$ cm; (b) $m = 50$, $S_{\text{g}} = 6$ cm; (c) $m = 300$, $S_{\text{g}} = 6$ cm; (d) $m = 300$, $S_{\text{g}} = 100$ cm. Through calculation, the PV, RMS and GRMS of each surface error curves can be obtained. And the specific value can be found in Fig. 2. The corresponding temporal contrast is shown in Fig. 2(e). As shown in Fig. 2(e), the temporal contrast declines fast when the values of PV, RMS and GRMS are large (Fig. 2(a)). But when the values of PV, RMS, and GRMS are reduced (Fig. 2(b)–(d)), the temporal contrast is becoming better and better.

In the further analysis, the surface error curves generated by Eq. (6) are by spatial filtering. Figures 3(a)–(d) plot surface errors curves of the optical elements are achieved by different spatial filtering in the stretcher and compressor, in which Fig. 3(a) is not spatial filtering,

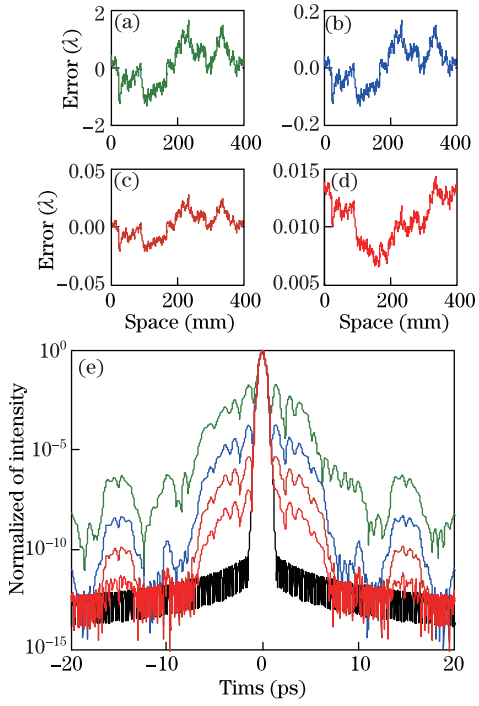

Fig. 2. (Color online) (a)–(b) Different surface error curves of the optical elements generated by random phase screen in the stretcher and compressor. (e) The temporal distribution of the normalized laser intensity corresponding to the surface error curves in (a)–(d), and the black curve is the value in ideal condition. (a) PV=3λ, RMS=0.65λ, GRMS=2λ cm^{-1}, (b) PV=λ/3, RMS=λ/15, GRMS=λ/4 cm^{-1}, (c) PV=λ/20, RMS=λ/93, GRMS=λ/30 cm^{-1}, and (d) PV=λ/127, RMS=λ/520, GRMS=λ/200 cm^{-1}.

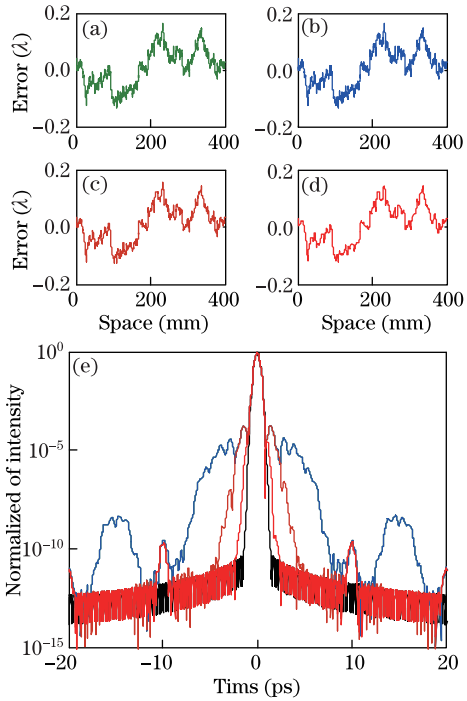

Fig. 3. (Color online) (a)–(d) Different surface error curves of the optical elements generated by spatial filtering in the stretcher and compressor; (e) temporal distribution of the normalized laser intensity corresponding to the surface error curves in (a)–(d), and the black curve is the value in ideal condition. (a) PV=$\lambda/3$, RMS=$\lambda/15$, GRMS=$\lambda/4$ cm^{-1}, (b) PV=$\lambda/3$, RMS=$\lambda/15$, GRMS=$\lambda/4$ cm^{-1}, (c) PV=$\lambda/3$, RMS=$\lambda/15$, GRMS=$\lambda/8$ cm^{-1}, and (d) PV=$\lambda/3$, RMS=$\lambda/15$, GRMS=$\lambda/12$ cm^{-1}.

Figs. 3(b), (c) and (d) are separately achieved by 0–10-μm, 0–120-μm, 0–33 mm scalelengths spatial filtering. And the original surface error curves of Fig. 3(a) is achieved by using following parameter $m = 50$, $S_g = 6$ cm. The corresponding temporal contrast is shown in Fig. 3(e). As shown in Fig. 3(e), when the surface error curves is by 0–10 μm scalelengths spatial filtering (as shown in Fig. 3(b)), the temporal contrast is the same value as without spatial filtering (as shown in Fig. 3(a)). And the temporal contrast is improved after 0–120 μm scalelengths spatial filtering (As shown in Fig. 3(c)). Further simulation indicates that, when the surface error curves is by 0–33 mm scalelengths spatial filtering (as shown in Fig. 3(d)), the temporal contrast is almost the same value as ideal condition (as shown in Fig. 3(e) black curve).

In conclusion, the temporal contrast degradation by the spectral phase distortion is studied in CPA lasers. We analyze the impact of the surface qualities of the optical elements such as mirrors and grating in the stretcher and compressor on the temporal contrast. Because the roughness of the surface is directly converted to the spectral phase distortion, which reduces the temporal coherence of the main pulse and generates a noisy structure on its sides. Simulation indicates that the temporal contrast declines fast in the case of a rapidly varying random surface error. And when the values of PV, RMS, and GRMS of the surface error curve are reduced, the temporal contrast is becoming better and better. Further simulation indicates that, the temporal contrast can be improved when the surface error curves after spatial filtering. Those results are helpful for the choice of the surface parameters of the optical elements in the stretcher and compressor.

This work was supported by the National "863" Program of China (No. 2010AA8044010), and the Youth Innovation Foundation of National Laboratory on High Power Laser and Physics, Shanghai Institute of Optics and Fine Mechanics, Chinese Academy of Sciences.

References

1. D. Strickland and G. Mourou, Opt. Commun. **56,** 219 (1985).
2. G. A. Mourou, T. Tajima, and S. V. Bulanov, Rev. Mod. Phys. **78,** 309 (2006).
3. A. Jullien, O. Albert, F. Burgy, G. Hamoniaux, L. P. Rousseau, J. P. Chambaret, F. Auge-Rochereau, G. Cheriaux, J. Etchepare, N. Minkovski, and S. M. Saltiel, Opt. Lett. **30,** 920 (2005).
4. H. Ren, L. Qian, H. Zhu, D. Fan, and P. Yuan, Opt. Express **18,** 12948 (2010).
5. C. Liu, Z. Wang, W. Li, Q. Zhang, H. Han, H. Teng, and Z. Wei, Opt. Lett. **35,** 3096 (2010).
6. Y. Huang, C. Zhang, Y. Xu, D. Li, Y. Leng, R. Li, and Z. Xu, Opt. Lett. **36,** 781 (2011).
7. S. Fourmaux, S. Payeur, S. Buffechoux, P. Lassonde, C. St-Pierre, F. Martin, and J. C. Kieffer, Opt. Express **19,** 8486 (2011).
8. K. H. Hong, B. Hou, J. A. Nees, E. Power, and G. A. Mourou, Appl. Phys. B **81,** 447 (2005).
9. G. Xu, T. Wang, Z. Li, Y. Dai, Z. Lin, Y. Gu, and J. Zhu, Rev. Laser Eng. (Suppl) 1172 (2008).
10. W. Williams, J. Auerbach, J. Hunt, L. Lawson, K. Manes, C. Orth, R. Sacks, J. Trenholme, and P. Wegner, *NIF Optical Phase Gradient Specification*, UCRL-ID-127297[R]. Lawrence Livemore National Laboratory, USA, 1997.